Molecular Immunology 190 (2026) 21–33

Contents lists available at ScienceDirect

Molecular Immunology

journal homepage: www.elsevier.com/locate/molimm

An H_2S-releasing oridonin derivative protects HaCaT cells against metabolic stress via PI3K/AKT/Nrf2 signaling

Lang Lin [a,1], Yuzhen Jia [a,1], Rubing Xue [a], Yutong Shi [a], Dahong Li [b], Fanxing Xu [a,*], Chun Chu [c,*]

[a] Wuya College of Innovation, Shenyang Pharmaceutical University, Shenyang 110016, PR China
[b] School of Traditional Chinese Materia Medica, Shenyang Pharmaceutical University, Shenyang 110016, PR China
[c] School of Basic Medicine, Shenyang Medical College, Shenyang 110034, PR China

ARTICLE INFO

Keywords:
Hydrogen sulfide
Oridonin
Keratinocyte apoptosis
PI3K/AKT/Nrf2 pathway
Diabetic wound healing

ABSTRACT

The chronic hyperglycemia and its-associated metabolic changes often lead to impaired wound healing, which seriously affects the quality of life of diabetic patients. Oxidative stress and apoptosis are key factors that impede epidermal cell proliferation and migration and delay wound healing. The aim of this study was to investigate the protective effect of a novel hydrogen sulfide (H_2S)-releasing oridonin derivative (OAc-Ph-ADT) on epidermal HaCaT cells against a high-glucose and high-fat environment *in vitro*. Mechanistic studies showed that OAc-Ph-ADT exerted its antioxidant effects by activating the PI3K/AKT/Nrf2 signaling pathway. Specifically, it increased PI3K and phosphorylated-AKT expression, and promotes Nrf2 nuclear translocation, which in turn enhances the mRNA and protein expression of downstream antioxidant factors (HO-1, SOD2 and NQO1). In addition, OAc-Ph-ADT significantly reduced apoptosis by inhibiting the decrease in mitochondrial membrane potential and decreasing the expression of apoptosis-related proteins (Bax, Cleaved-Caspase 3/9). It was also observed that OAc-Ph-ADT up-regulated the expression of cystathionine β-synthase (CBS) via Nrf2, which further promoted the synthesis of endogenous H_2S, resulting in positive feedback regulation. In summary, this paper elucidated through systematic *in vitro* experiments that OAc-Ph-ADT has a protective effect against epidermal cell damage in a high-glucose and high-fat environment, revealing its potential as a candidate molecule for diabetic wound treatment, and this novel H_2S-releasing oridonin derivative has a potential application as a diabetic wound healing promoter.

1. Introduction

Diabetes is a metabolic disorder characterized by chronic hyperglycemia. Poor long-term blood glucose control can lead to damage to multiple systems, including the eyes, kidneys, nerves, and cardiovascular system (Schlienger, 2013). Among all types of diabetes, type 2 diabetes (T2DM) accounts for more than 90 % of cases and is the primary type of diabetes in China and globally. T2DM is closely related to a high-glucose, high-fat diet, with obesity and insulin resistance being important contributing factors (Zhang et al., 2022). A high-glucose, high-fat environment can also disrupt metabolic processes and impair wound healing. Poor wound healing reduces their quality of life and overall health (Agostinis et al., 2021; Mohan et al., 2019). Oxidative stress causes the accumulation of reactive oxygen species (ROS), which restrain cellular repair, replication, and migration (Khodr, Khalil, 2001). In diabetic patients, elevated apoptosis, driven by oxidative stress and inflammation, reduces wound repair and restricts new tissue formation, thereby slowing wound healing (Jin et al., 2018). The hyperglycemic state in diabetic patients significantly impairs the function of epithelial cells in wound healing. Hyperglycemia-induced oxidative stress and accumulation of advanced glycosylation end products (AGEs) inhibit the migration and proliferation ability of keratinocytes, slowing down the process of epithelial re-formation (Lan et al., 2008). Meanwhile, the persistent inflammatory microenvironment leads to excessive release of pro-inflammatory factors (e.g., TNF-α and IL-1β), which further disrupts the epithelial repair signaling pathway. In addition, aberrant activation of matrix metalloproteinase (MMP-9) excessively degrades the extracellular matrix and prevents normal reconstruction of the epithelial layer. To address these dysfunctions, current research strategies include the application of Nrf2 activators (e.g., curcumin) as direct or indirect

* Corresponding authors.
E-mail addresses: fanxing0011@163.com (F. Xu), chuchuphd@163.com (C. Chu).
[1] These authors contributed equally to this work

https://doi.org/10.1016/j.molimm.2025.12.012
Received 3 September 2025; Received in revised form 14 December 2025; Accepted 19 December 2025
Available online 2 January 2026
0161-5890/© 2025 Elsevier Ltd. All rights are reserved, including those for text and data mining, AI training, and similar technologies.

antioxidants to mitigate oxidative stress damage (Duan et al., 2022), and the use of a hydrogen sulfide (H_2S)-releasing multifunctional hydrogel dressing (DATS@PFC&CMC) to improve the local microenvironment (Chen et al., 2023).

Oridonin, a bioactive compound extracted from *Rabdosia rubescens* (Hemsl.) Hara, exhibits various pharmacological effects such as anti-inflammatory, anti-tumor, and immunomodulatory activities (Song et al., 2018). Oridonin activates the nuclear factor E2-related factor 2 (Nrf2) signaling pathway, attenuates oxidative stress-induced injuries of endothelial cells (Li et al., 2021). This mechanism is essential for tissue regeneration and repair during wound healing. Through its "pleiotropic" effects of anti-inflammatory, antioxidant, and modulation of key proliferation/migration pathways, oridonin may be a potential candidate for promoting re-epithelialization, especially in chronic wounds. However, the hydrophobicity of oridonin restricts its bioavailability, driving researchers to modify its structure to improve solubility and bioavailability (Zhang et al., 2020).

H_2S promotes rapid and effective wound healing (Qian et al., 2020). Two strategies exist for utilizing H_2S to enhance wound healing include promoting endogenous H_2S release and supplying exogenous H_2S supplementation. Optimal H_2S concentrations offer several biological benefits, including downregulation of oxidative stress, inflammation and apoptosis (Kabil et al., 2014). In terms of inhibiting oxidative stress, H_2S not only directly scavenges ROS, but also up-regulates endogenous antioxidant defense systems such as superoxide dismutase (SOD) and glutathione (GSH) (Calvert et al., 2009; Corsello et al., 2018; Hassan et al., 2012; Peake et al., 2013; Xie et al., 2016; Zhou et al., 2014). Its anti-inflammatory effects were mainly achieved by inhibiting the activation of the NF-κB signaling pathway and NLRP3 inflammatory vesicles, which significantly reduced the production of pro-inflammatory factors such as TNF-α and IL-6 (Huerta de la Cruz et al., 2022; Zhang et al., 2024). In terms of anti-apoptosis, H_2S effectively protects cells from apoptosis by regulating the Bcl-2/Bax ratio, inhibiting caspase-3 activation, and activating pro-survival signaling pathways such as PI3K/Akt (Cheng et al., 2016; Mironov et al., 2017). NaHS and Na_2S have been widely used for exogenous H_2S supply, but their short half-life and rapid, uncontrolled release of H_2S make them unsuitable for sustained supply of H_2S (Powell et al., 2018). Compared to the traditional donor NaHS, ADT has sustained-release properties and maintains a more stable therapeutic concentration of H_2S, while avoiding the cytotoxicity associated with NaHS at high concentrations (Cai et al., 2020). ADT-based H_2S therapy can significantly promote wound healing, inhibit scarring, enhance revascularization, and protect residual neurons and axons from secondary damage. ADT is also effective in improving high-fat diet-induced fatty acid metabolism disorders and liver injury. Cystathionine-β-synthase (CBS) is an essential enzyme for endogenous H_2S and persulfide biosynthesis, with its activity directly regulating H_2S production (Czikora et al., 2022; Scheid et al., 2021). CBS catalyzes the condensation of L-cysteine and homocysteine to produce cystathionine (which can subsequently be metabolized by CSE to produce H_2S). Studies have shown that CBS-mediated H_2S production plays an important role in physiological processes, such as cardioprotection, neuromodulation and anti-inflammation (Szabo, 2016). Recent studies have found that aberrant CBS expression is closely associated with a variety of diseases such as non-alcoholic fatty liver disease and cancer (Werge et al., 2021; Zhu et al., 2018), making it a potential target for drug intervention.

In recent years, researchers have developed H_2S-releasing natural products derivatives through structural modification (Li et al., 2019; Li et al., 2024; Li et al., 2020; Wang et al., 2023). These derivatives not only improve the hydrophobicity of natural products and enhance its bioavailability but also utilize the physiological regulatory functions of H_2S, such as anti-inflammatory, anti-tumor, and antioxidant effects, further enhancing the biological activity of natural products and H_2S. H_2S-releasing oridonin conjugates, created by linking oridonin with H_2S donors like ADT-OH or α-lipoic acid, demonstrate dual efficacy, offering enhanced anti-tumor ability (Li et al., 2024). These derivatives hold promise for application as nutritional supplements, serving as dietary supplements that leverage the advantages of both medicinal and edible properties to assist in improving wound healing in diabetes.

In the current study, a high-glucose, high-fat environment was constructed to culture epithelial cell line HaCaT cells. Based on the the effects on proliferation of HaCaT cells and H_2S-releasing activity, the lead candidate was screened from 21 pre-synthesized H_2S-releasing oridonin derivatives (Li et al., 2019, 2020). The impacts of the compound on cell migration, apoptosis and ROS levels regulated by the PI3K/AKT/Nrf2 pathway was further evaluated. This new class of potential drugs was found to reduce oxidative stress associated with impaired wound healing and to promote endogenous H_2S synthesis.

2. Materials and methods

2.1. HaCaT cell culture

HaCaT were obtained from the Cell Resource Center of the Shanghai Institutes for Biological Sciences, Chinese Academy of Sciences. The cells were cultured in an incubator at 37 °C with 5 % CO_2 using high glucose DMEM (Gibco, 12800017) containing 10 % FBS (Procell, 164210-Z), 100 U/mL penicillin and 100 μg/mL streptomycin .

2.2. Viability assay

HaCaT cells were inoculated into 96-well plates at a density of 1×10^4 cells per well and cultured for 24 h at 37 °C in a 5 % CO_2 incubator. The setup groups were PA, OAc-Ph-ADT, PA + Oridonin and PA + ADT-OH, and then the cells were exposed to DMEM with a concentration of 0.5 μM compound for 24 h. After the processing is completed, the wells were then washed once with PBS, and serum-free culture medium containing 10 % (v/v) CCK-8 (Meilun, ma0225–1) was added to each well. The cells were subsequently incubated for 2 h. Absorbance at 450 nm was measured using a microplate reader to assess the viability of HaCaT cells.

2.3. H_2S release test

Quantification of H_2S release by the Methylene Blue Plus (MB+) method, which is based on the reaction of H_2S with a specific reagent to form methylene blue, which is quantified by measuring its characteristic absorbance at 670 nm (Li, 2015). Standard solutions of Na_2S were prepared in 50 mL volumetric flasks at concentrations of 5, 10, 20, 40, 60, 80, 100, and 150 μM. The standard solution (1 mL) of each concentration was added to a mixture of methylene blue method consisting of 200 μL of 1.2 M hydrochloric acid solution containing 30 mM ferric chloride, 200 μL of 7.2 M hydrochloric acid solution containing 20 mM N,N-dimethyl-p-phenylenediamine hydrochloride, and 100 μL of an aqueous solution containing a mass concentration of 1 % zinc acetate, and then left at room temperature for 20 min. The cuvette was positioned in a UV–visible spectrophotometer, where the absorbance was recorded at a wavelength of 670 nm, and a Na_2S standard curve was constructed (Xu et al., 2019). NaHS or each conjugate was dissolved in tetrahydrofuran to make a tetrahydrofuran solution of conjugate at a concentration of 40 mM. After adding 1 mM of L-cysteine in PBS as a pro-release agent, the previously made tetrahydrofuran solution of the conjugates was added and stirred at room temperature. Finally, after 20 min of standing at room temperature, the samples from different groups were transfered to 96-well plates and the absorbance weas measured at 670 nm. The amount of H_2S released was calculated from a standard curve based on the absorbance of each compound.

2.4. Quantitative determination of ROS

HaCaT cells were inoculated in 96-well plates and treated with

different concentrations of drugs for 24 h, followed by the incubation with a 10 μM of DCFH-DA (Beyotime, s0033) probe solution for 30 min at 37 °C in the dark. The effect of different concentrations of PA on ROS production was measured by the absorbance of cell suspension using a fluorescence enzyme marker at 530 nm. The cells were washed three times with PBS and subsequently stained with DCFH-DA probe solution at a dilution of 1:1000. The cells were incubated at 37 °C for 30 min, resuspended in 300 μL of PBS, passed through a sieve, and analyzed for the effect of OAc-Ph-ADT on ROS generation using flow cytometry

2.5. MDA, GSH, and SOD assay

HaCaT cells were treated with indicated compounds, and incubated for 24 h. Subsequent assays were conducted using MDA (NanJing Jiancheng Bio, A003–1–2), GSH (NanJing Jiancheng Bio, A006–2-1), and SOD assay kits (NanJing Jiancheng Bio, A001–1). Absorbance values were then measured using an enzyme marker at wavelengths of 532 nm, 405 nm, and 450 nm, respectively, to evaluate the effect of OAc-Ph-ADT on intracellular levels of MDA, GSH, and SOD.

2.6. Western blot analysis

HaCaT cells were collected and washed twice with cold PBS, then lysed with RIPA buffer containing 1 % PMSF. The lysate was centrifuged at 15,000 × g for 10 min, and the supernatant was used for western blot analysis. Proteins were separated using 10 % and 12 % SDS-PAGE and subsequently transferred to PVDF membranes. After blocking with 5 % skimmed milk powder in TBST (0.1 % Tween 20) for 2 h at room temperature, all blots were incubated overnight at 4 °C with the following primary antibodies: Nrf2 (Proteintech, 60225–1), Keap1 (Santa Cruz, sc-514914), HO-1 (Proteintech, 66743–1), NQO-1 (Proteintech, 18985–1-AP), SOD2 (Proteintech, 83519–3), mTOR (Huaan Bio, ET1608–5), Bax (Huaan Bio, ET1603–34), Bcl-2 (Abmart, T40056), PI3K (Huaan Bio, ET1608–70), p-AKT (Huaan Bio, ET1607–73), β-actin (Proteintech, 66009–1) and β-tubulin (Proteintech, 10068–1-AP). The secondary antibodies conjugated with HRP were added to the blots, the signal was excited using ECL luminous solution, and the results were captured by a gel imager. All data were normalized as the optical density ratio between the target protein and the internal control protein (β-actin/β-tubulin). The protein band images obtained from photography were quantitatively analyzed using Image J software to calculate the relative expression level of each protein.

2.7. qRT-PCR analysis

HaCaT cells were cultured and pretreated with different compounds for 24 h or with siRNA. Total RNA was extracted with an RNA extraction kit. cDNA was synthesized using a reverse transcription kit (SevenFast® Two Step RT&qPCR Kit, SRQ-01). qRT-PCR was subsequently performed as follows: initial denaturation at 95 °C for 30 s, 40 cycles at 95 °C for 5 s; 55 °C for 15 s; and 72 °C for 10 s. GAPDH served as the endogenous control. The results were analyzed using the $^{\Delta\Delta}$Ct method. The primer sequences used in this study are provided in Table 1.

Table 1
List of primers sequences used for qPCR experiments.

Genes	Forward/Reverse
CBS	Forward: GGCCAAGTGTGAGTTCTTCAA Reverse: GGCTCGATAATCGTGTCCCC
SOD2	Forward: GTGGAGAACCCAAAGGGGAGTT Reverse: GTGGAATAAGGCCTGTTGTTCCTT
HO-1	Forward: AACTTTCAGAAGGGCCAGGT Reverse: AGACTGGGCTCTCCTTGTTG
NQO1	Forward: AGTGGCATCCTGCGTTTCT Reverse: GGATACTGAAAGTTCGCAGGG
GAPDH	Forward: GAAGAGCACTGATCGTACTGGC Reverse: TCTCGCTCCTGGAAGATGGTG

2.8. siRNA transfection

Target gene siRNA and the negative control Non-specific Control (NC) siRNA (Table 2) was diluted to a concentration of 10 nM using buffer. A 2.4 μL of transfection reagent was added to 100 μL of the above solution, mixed thoroughly, and incubated at room temperature for 20 min. The incubated reagent was then added to HaCaT cells cultured in Opti-MEM. After 6 h, the Opti-MEM medium containing the transfection reagent and replaced with regular medium for continued culture for 48 h. The knockout efficiency of target gene was evaluated using Western blot analysis.

2.9. Immunofluorescence assay

HaCaT cells were treated with different compounds for 24 h, and were collected and permeabilized in 0.5 % Triton-X for 10 min. The cells were subsequently blocked with 3 % BSA for 2 h at room temperature and incubated overnight at 4 °C with 150 μL of diluted Nrf2 (1:200, Proteintech, 16396–1-AP) primary antibody. The cells were washed with PBS, incubated with fluorescein isothiocyanate-labelled secondary antibody (Proteintech, RGAM001) for 2 h in the dark and stained with DAPI for 10 min. Finally, the cells were observed under a confocal fluorescence microscope (Nikon, Tokyo).

2.10. Scratch assay

HaCaT cells were inoculated into 6-well plates, and 3 vertical scratches were made parallel to the transverse direction of the wells using a 200 μL pipette tip with uniform and steady force, ensuring clear and intact edges for subsequent observation and analysis. Preformulated serum-free medium containing different concentrations of drugs was added to each culture well. The cell migration process was observed and recorded at 0, 6, 12, and 24 h at the same location using an inverted microscope. The cells scratch area was calculated using Image J software. The cell migration rate was calculated using the formula:

$$\text{Cell migration}(\%) = \frac{S_{0h} - S_{24h}}{S_{0h}} \times 100$$

2.11. Detection of apoptosis by Annexin-V FITC/PI double staining assay

HaCaT cells were inoculated into 6-well culture plates at a density of 2×10^5/well for 24 h. After treatment, Annexin V-PI (Beyotime, BA1120) staining reagent was added according to the instructions, and the reaction was carried out for 15 min in the dark. The fluorescence intensities of FITC and PI were evaluated using a flow cytometer (Becton Dickinson, USA) to detect cell death. The cell sorting strategy is as follows: First, delineate the main cell population in the forward scatter (FSC-A) versus side scatter (SSC-A) scatter plot to exclude debris and dead cells. Subsequently, in the Annexin V-FITC and PI fluorescence channel scatter plots, quadrant gates were established based on positive and negative controls to distinguish live cells (Annexin V^-/PI^-), necrotic cells (Annexin V^-/PI^+), early apoptotic cells (Annexin V^+/PI^-), and late apoptotic/necrotic cells (Annexin V^+/PI^+).

Table 2
List of Nrf2 siRNA sequence.

Target gene	siRNA sequence
Nrf2	Sense: UGGAUUUGAUUGACAUACUUUGG Antisense:CCAAAGUAUGUCAAUCAAAUCCA

2.12. JC-1 staining for mitochondrial membrane potential detection

Cells were treated with drugs for 24 h, and then were collected and stained according to the JC-1 kit instructions (Meilun, mb12531). The fluorescence changes of the JC-1 monomer (Ex/Em, 488/525 nm) and JC-1 aggregates (Ex/Em, 543/590 nm) were observed using a fluorescence microscope.

2.13. Statistical analysis

GraphPad Prism 8.0 was used to statistically analyze all data, and all experimental results were obtained from independent experiments with 3 replicates. First, the Shapiro-Wilk test was used to assess normality of distribution. With data met the criteria for normality, one-way analysis of variance (ANOVA) was performed, followed by Dunnett's test for multiple comparisons The results were considered statistically significant at $P < 0.05$.

3. Results

3.1. H_2S releasing oridonin derivative promotes cell proliferation and migration of HaCaT cells

We selected PA to simulate a high-fat environment, and a high glucose concentration of 30 mmol/L to simulate a high-glucose environment, this glucose concentration has been widely used and validated in the *in vitro* studies of HaCaT cells under high-glucose conditions (Zhang, Chen, 2022). HaCaT cells were exposed to PA at concentrations ranging from 100 to 600 μM and high level of glucose at a concentration of 30 mmol/L for 24 h. The CCK-8 was used to test the effect of PA on HaCaT cell viability (Fig. S1), and the results indicated that the concentration of 300 μM led to a decrease in cell viability by approximately 50 %. We selected 300 μM PA and 30 mmol/L glucose as the optimal conditions for the following experiments. The levels of ROS in HaCaT cells in a high-glucose and high-fat environment were determined, and ROS levels were shown to be increased with increasing PA concentration (Fig. S2), indicating that PA was associated with an increase in ROS levels during the induction of cell damage.

A series of pre-synthesized H_2S-releasing oridonin derivatives were screened by CCK-8 assay, and the results showed that the derivative numbered 2 (named OAc-Ph-ADT) was superior to the other compounds, and showed greater efficacy than either ADT-OH or oridonin alone in terms of effectively mitigating the effect of the high-glucose and high-fat environment on the viability of the cells (Fig. 1A and B). The EC_{50} value of OAc-Ph-ADT was determined to be 2.919 μM (Fig. S3A). Then we selected different concentrations of OAc-Ph-ADT to evaluate its effect on HaCaT cell viability (Fig. S3B). Results indicated that within the selected 0–50 μM concentration range, OAc-Ph-ADT had no significant impact on HaCaT cell viability. To determine the H_2S release capacity of each derivative, the study used the MB+ for H_2S quantification. The results indicated that the amount of H_2S release gradually increased with time and peaked within 15–20 min (Fig. 1C). This suggests that all derivatives were able to steadily release H_2S. In particular, OAc-Ph-ADT exhibited a higher H_2S release capacity of 18–20 μM. To characterize the H_2S release kinetics of OAc-Ph-ADT, we compared it with the standard donor NaHS. As shown in Fig S4, NaHS predictably triggered an explosive increase in H_2S concentration immediately upon addition, reaching a peak within a short timeframe before rapidly declining. In contrast, OAc-Ph-ADT exhibited a mild and sustained release pattern. This controlled, non-burst release kinetics of OAc-Ph-ADT may better align with the drug release behavior requirements for an ideal wound treatment agent. Additionally, quantitative analysis of the scratch assay revealed that, compared to the untreated group, the wound closure rate of cells treated with OAc-Ph-ADT increased in a dose-dependent manner after 24 h. The migration area in the 5 μM OAc-Ph-ADT-treated group was significantly superior to that of the oridonin group and the ADT-OH group at the same concentration. (Fig. 1D and E). Based on these data, we selected 5 μM OAc-Ph-ADT for subsequent experiments.

3.2. OAc-Ph-ADT attenuates high glucose and high fat-induced apoptosis in HaCaT cells

Apoptosis of keratinocytes is a key factor in impaired re-epithelialization of diabetic wounds. Inhibition of the Nrf2 signaling pathway leads to decreased expression of its downstream antioxidant genes (HO-1), exacerbating apoptosis of keratinocytes in a high-glucose environment (O'Rourke et al., 2024). Meanwhile, MMP9 further promotes keratinocyte apoptosis through activation of the FasL/Fas signaling pathway, which together lead to delayed diabetic wound healing (Liang et al., 2019). Determined by AnnexinV-FITC/PI flow cytometry and TUNEL assay, the level of apoptosis in HaCaT cells was found to be elevated a high-glucose and high-fat environment, which was reversed by OAc-Ph-ADT (Fig. 2A and B, Fig. S5 and S6). A decrease in mitochondrial membrane potential is considered a classical feature of the apoptotic process. Results obtained using JC-1, a fluorescent dye commonly used for detecting the mitochondrial membrane potential, indicated that OAc-Ph-ADT was able to restore the reduction in mitochondrial membrane potential induced by the high-glucose and high-fat environment (Fig. 2C and D). Moreover, changes in the ratio of apoptosis-regulating proteins, including Bcl-2, Bax, Caspases 3 and Caspase 9 were detected. The results revealed that the ratios of cleaved Caspase 9/Caspase 9 as well as cleaved Caspase 3/Caspase 3 were increased and the ratio of Bcl-2/Bax was decreased in HaCaT cells under high-glucose and high-fat environments (Fig. 2E-J). In contrast, the results of the above experiments were reversed by the addition of OAc-Ph-ADT. This suggests that OAc-Ph-ADT is able to regulate the expression of apoptosis-related proteins under high glucose and high fat environments, and thus plays a role in inhibiting apoptosis in HaCaT cells.

3.3. OAc-Ph-ADT reduced PA-induced oxidative stress in HaCaT cells

Oxidative stress leads to excessive accumulation of ROS in epithelial cells, triggering oxidative damage to lipids, proteins, and DNA, disrupting cellular homeostasis and promoting inflammatory responses (Sies et al., 2017). The antioxidant effect of OAc-Ph-ADT on HaCaT cells against damage caused by the high-glucose and high-fat environment was evaluated. The results revealed that OAc-Ph-ADT could reverse the PA-induced elevation of ROS levels in HaCaT cells, which was superior to that of oridonin or ADT-OH alone (Fig. 3A). Biomarkers related to oxidation were assayed to determine the antioxidant capacity of OAc-Ph-ADT. The results showed that OAc-Ph-ADT treatment alleviated elevated MDA levels and up-regulated SOD levels (Fig. 3B and C). Additionally, OAc-Ph-ADT had a positive effect on intracellular GSH expression in HaCaT cells (Fig. 3D and S3B). These findings suggest that OAc-Ph-ADT may enhance cellular antioxidant capacity and reduce ROS-induced cellular damage by increasing the synthesis of GSH and SOD.

3.4. OAc-Ph-ADT activates the Nrf2 antioxidant pathway in HaCaT cells

ROS levels are tightly controlled by an inducible antioxidant program in response to cellular stressors and are mainly regulated by the transcription factor Nrf2 (DeNicola et al., 2011). Immunofluorescence results showed that the high-glucose and high-fat environment inhibited the intranuclear translocation of Nrf2, whereas OAc-Ph-ADT increased the intranuclear level of Nrf2 (Fig. 4A and B). Western blot results also showed that OAc-Ph-ADT, along with oridonin and ADT-OH, enhanced the protein content of Nrf2 in the nucleus (Fig. 4C and D). These findings suggest that OAc-Ph-ADT ameliorates the inhibition of Nrf2 translocation into the nucleus and promotes the activation of Nrf2 in the

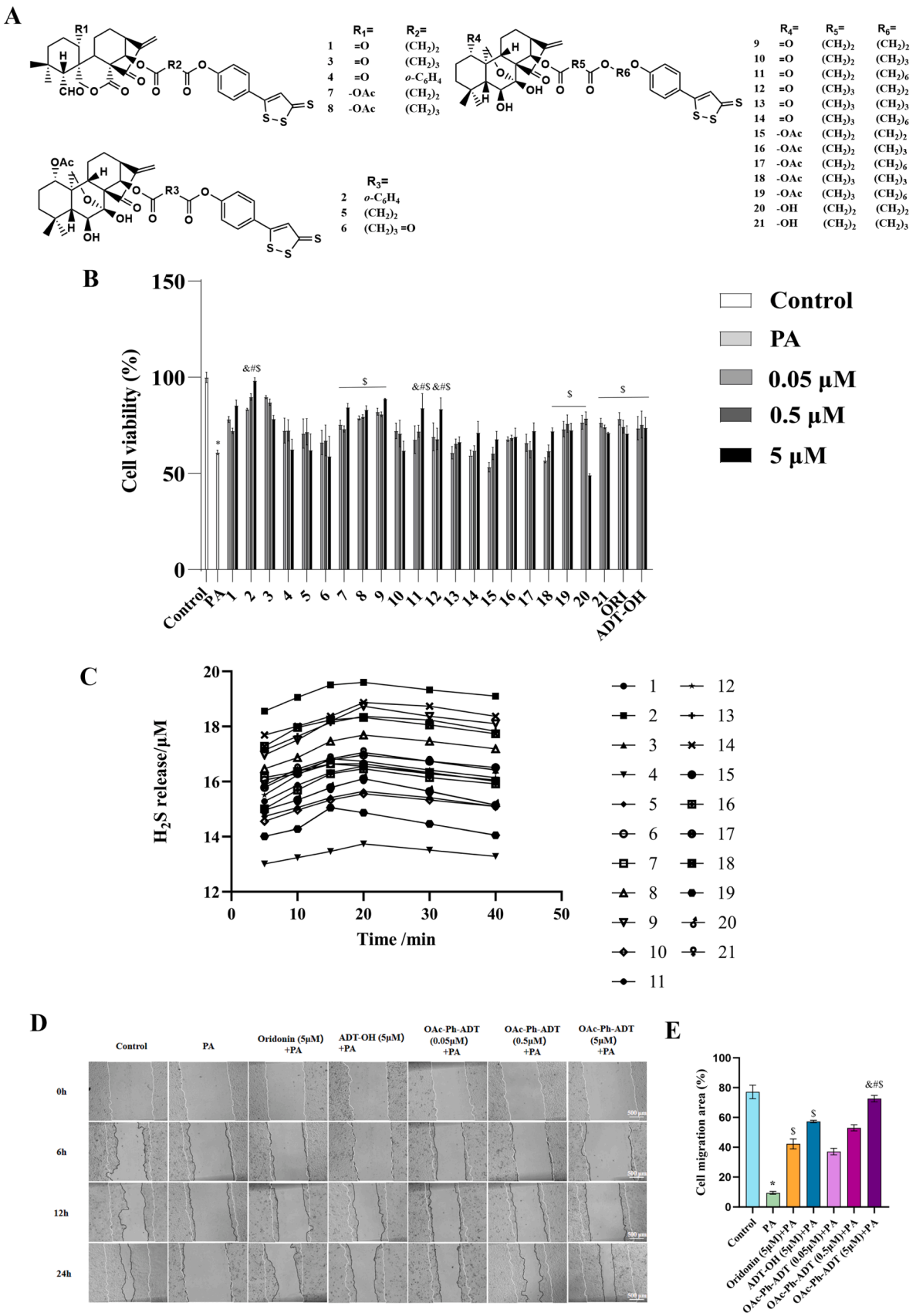

Fig. 1. The H_2S-releasing oridonin derivative capable of releasing H_2S and promoting the proliferation and migration of HaCaT cells. (A) Structure of H_2S-releasing oridonin derivatives. (B) Effects of different H_2S-releasing oridonin conjugates were determined on HaCaT cell viblility by CCK8. (C) *In vitro* H_2S release behavior of derivatives 1–21. (D, E) Cell migration scratch assay of HaCaT cells after 6, 12, and 24 h treatment. All results were expressed as the mean ± SD of three independent experiments. $^{*}P < 0.05$ versus control group; $^{\$}P < 0.05$ versus PA group; $^{\&}P < 0.05$ versus Oridonin + PA group; $^{\#}P < 0.05$ versus ADT-OH + PA group.

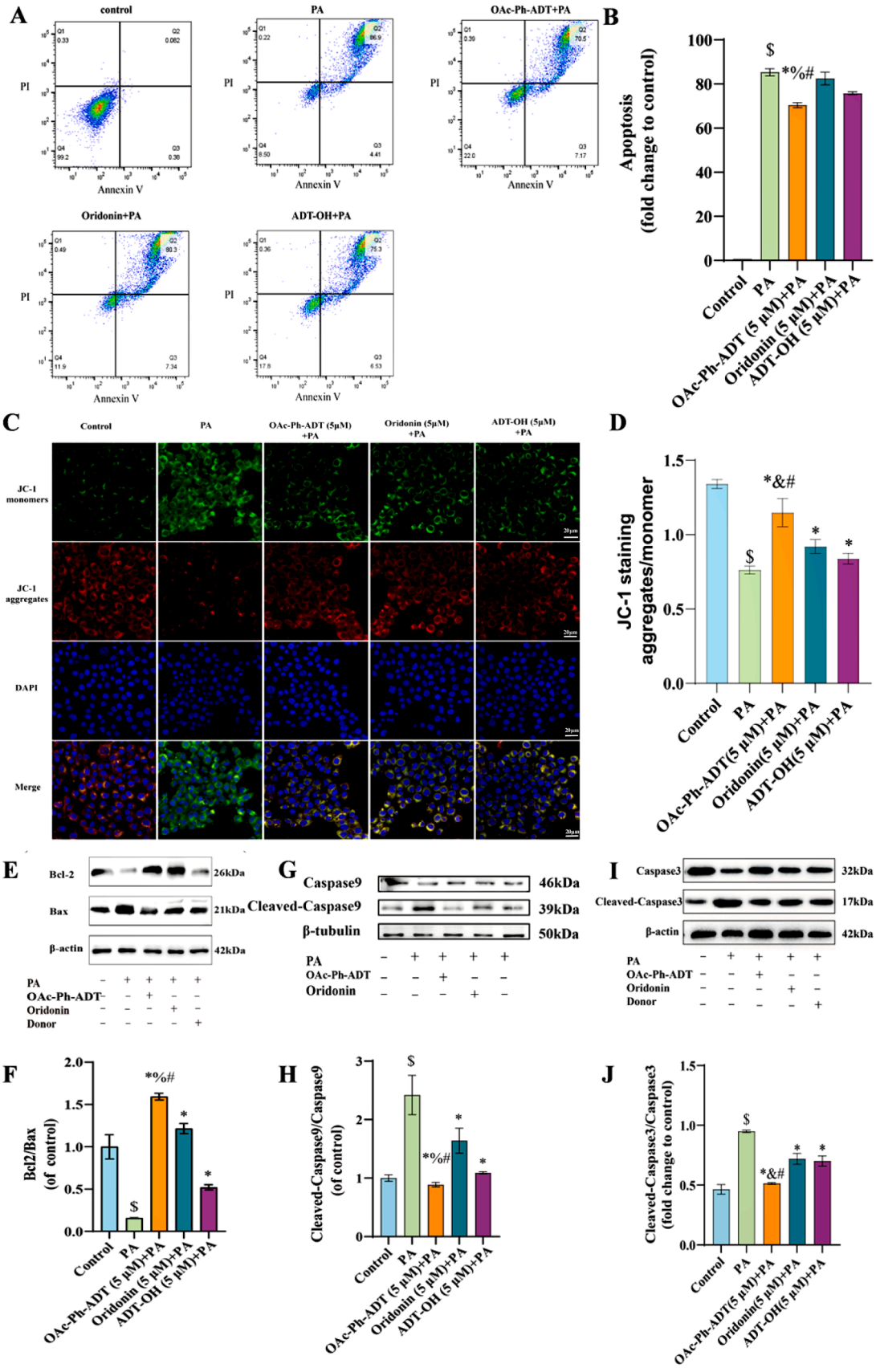

(caption on next page)

Fig. 2. Anti-apoptotic effects of OAc-Ph-ADT in HaCaT cells. (A-B) Apoptosis of OAc-Ph-ADT in HaCaT cells analyzed by flow cytometry and Annexin V-FITC/PI treated with different groups. (C, D) OAc-Ph-ADT (5 μM) on mitochondrial membrane potential in HaCaT cells was detected by immunofluorescence assay. Scale bar= 20 μm. (E, F) Western blot analyzing of the expression of Bcl-2, Bax in HaCaT cells, and the data were normalized as the optical density ratio between the target protein and the internal control protein β-actin. (G, H) Western blot analyzing of the expression of Caspase 9, Cleaved-Caspase 9 in HaCaT cells, and the data were normalized as the optical density ratio between the target protein and the internal control protein β-tubulin. (I, J) Western blot analyzing of the expression of Caspase 3, Cleaved-Caspase 3 in HaCaT cells, and the data were normalized as the optical density ratio between the target protein and the internal control protein β-actin. All results were expressed as the mean ± SD of three independent experiments. $^{\$}P < 0.05$ versus Control group; $^{*}P < 0.05$ versus PA group; $^{\&}P < 0.05$ versus Oridonin + PA group; $^{\#}P < 0.05$ versus ADT-OH + PA group.

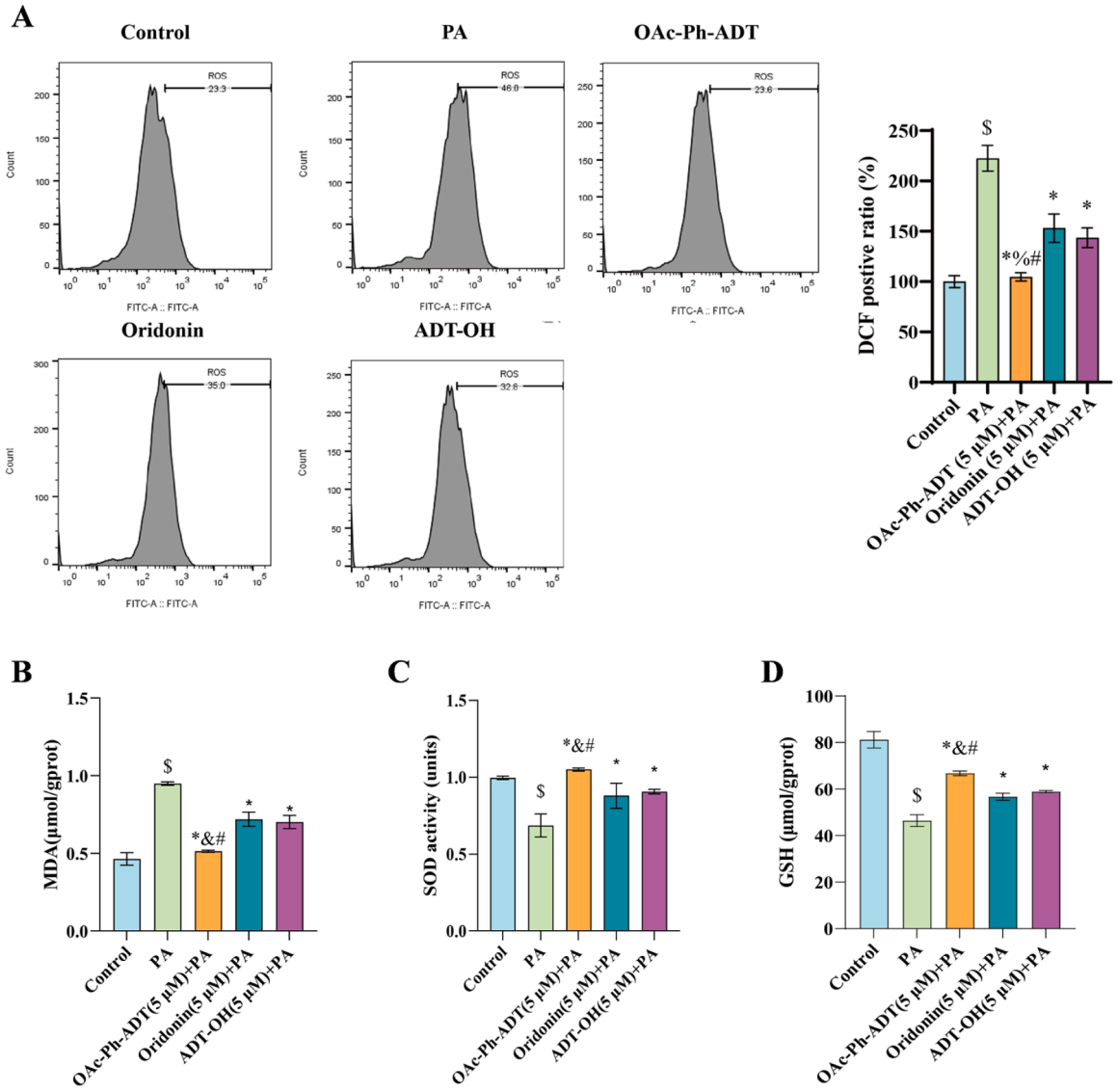

Fig. 3. Antioxidant effects of OAc-Ph-ADT in HaCaT cells. (A) OAc-Ph-ADT (5 μM) on ROS levels by flow cytometry. (B-D) OAc-Ph-ADT (5 μM) on MDA, SOD and GSH levels in HaCaT cells using commercialized kits. All results were expressed as the mean ± SD of three independent experiments. $^{\$}P < 0.05$ versus Control group; $^{*}P < 0.05$ versus PA group; $^{\&}P < 0.05$ versus Oridonin + PA group; $^{\#}P < 0.05$ versus ADT-OH + PA group.

cytoplasm, facilitating its translocation to the nucleus under high-glucose and high-fat environment. mRNA levels of HO-1, NQO1, and SOD2 were further assessed after treatment with OAc-Ph-ADT (Fig. 4E). Their mRNA levels were reduced in the PA group compared to the control group, while OAc-Ph-ADT increased the expression of NQO1, HO-1 and SOD2, which were higher than that of oridonin or ADT-OH alone. Additionally, OAc-Ph-ADT elevated the protein expression levels of these antioxidant factors (Fig. 4F-I). The results indicated that OAc-Ph-ADT up-regulated both mRNA and protein expression of antioxidant factors by promoting the intranuclear translocation of Nrf2.

3.5. OAc-Ph-ADT activates the PI3K/AKT/Nrf2 pathway in HaCaT cells

The PI3K/AKT pathway is a multifunctional classic signaling pathway associated with cell proliferation, anti-apoptosis and cell defense (He et al., 2021). OAc-Ph-ADT was found to upregulate the expression of PI3K, thereby increased p-AKT protein levels (Fig. 5A and B). We further investigated the effect of OAc-Ph-ADT on mTOR and GSK3β expression, which is a downstream effector of the PI3K-AKT signaling pathway involved in mediating cell survival and proliferation. The results indicated that OAc-Ph-ADT could upregulate the expression of mTOR and p-GSK3β (Fig. 5C-F). To investigate the role of

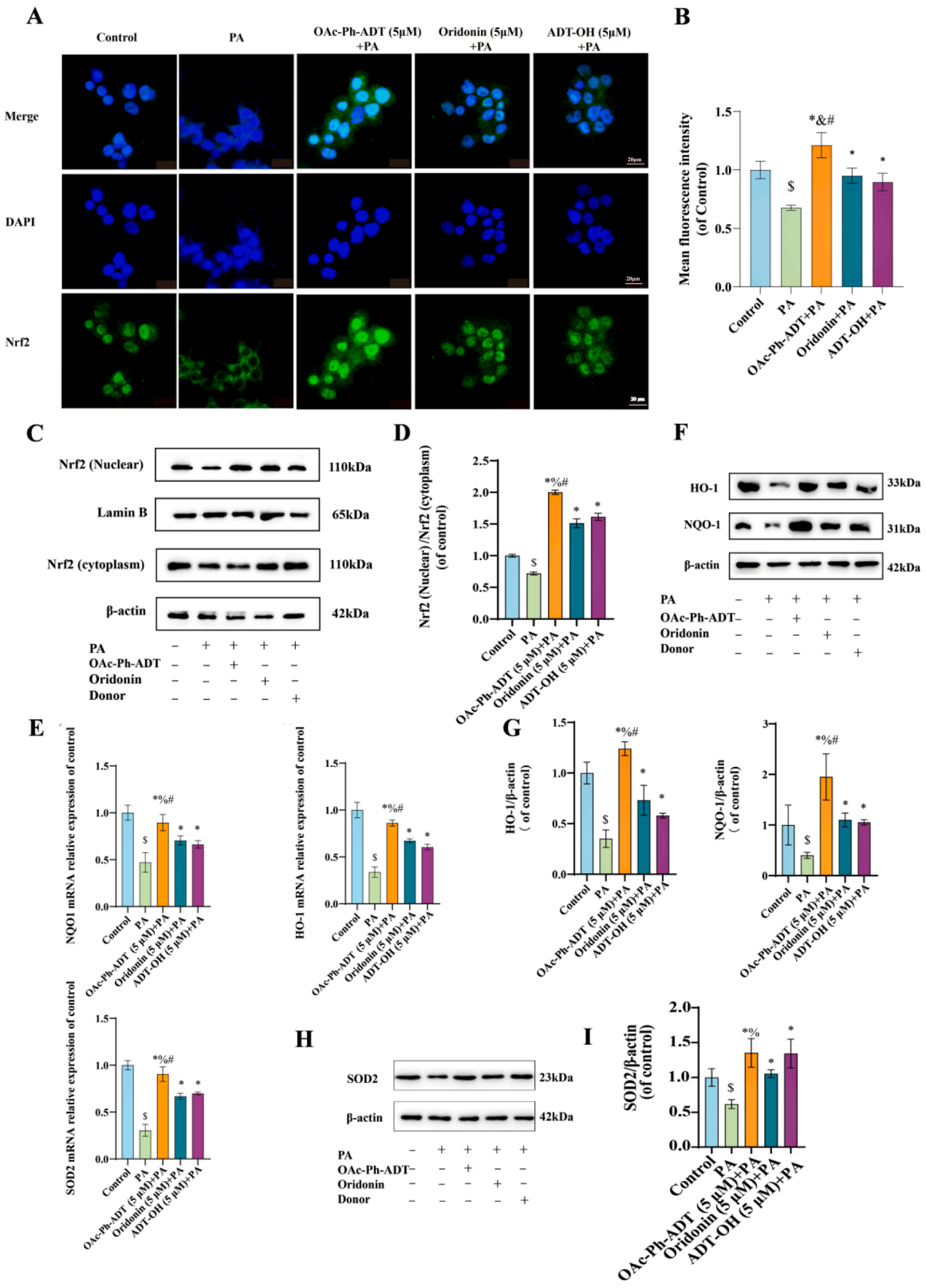

Fig. 4. OAc-Ph-ADT promotes intranuclear translocation of Nrf2 and increases levels of its downstream antioxidant factors in HaCaT cells. (A, B) Immunofluorescence staining of Nrf2 by confocal microscopy of HaCaT cells. (C, D) Western blot analysis of Nrf2 cytoplasm and nuclear protein expression in different groups. (E) qPCR analysis of NQO1 , HO-1 and SOD2 mRNA levels in different groups. (F-I) Western blot analysis of SOD2, HO-1 and NQO1 protein expression in different groups. All data of western blotting assay were normalized as the optical density ratio between the target protein and β-actin. All results were expressed as the mean ± SD of three independent experiments. $^{\$}P < 0.05$ versus Control group; $^{*}P < 0.05$ versus PA group; $^{\%}P < 0.05$ versus Oridonin + PA group; $^{\#}P < 0.05$ versus ADT-OH + PA group.

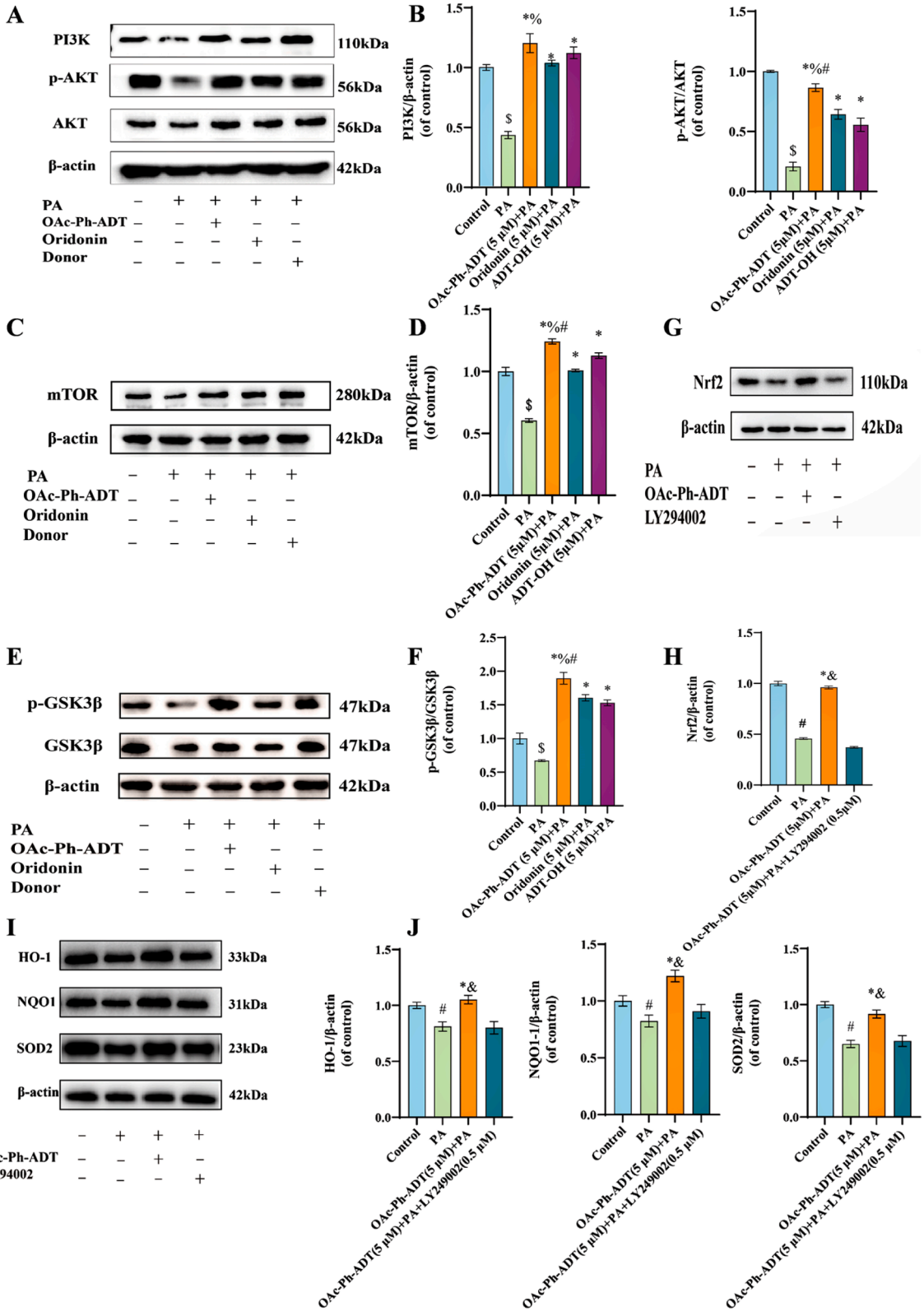

Fig. 5. Ac-Ph-ADT affects the PI3K/AKT/Nrf2 pathway in HaCaT cells. (A-F) Western blot was used to analyze of PI3K, AKT, p-AKT, mTOR, GSK3β and p-GSK3β protein levels in different groups. (G-J) LY294002 was added and Western bolt was used to analyze Nrf2 and its downstream HO-1, NQO1 and SOD2 protein expression in different groups. All data were normalized as the optical density ratio between the target protein and β-actin. All results were expressed as the mean ± SD of three independent experiments. $^{\$}P < 0.05$ versus Control group; $^{*}P < 0.05$ versus PA group; $^{\%}P < 0.05$ versus Oridonin + PA group; $^{\#}P < 0.05$ versus ADT-OH + PA group; $^{\&}P < 0.05$ versus Conjugate+ PA+ LY294002 group.

the PI3K/AKT pathway on antioxidant effect of OAc-Ph-ADT, LY294002 was co-incubated with OAc-Ph-ADT in HaCaT cells. The results showed that the elevated Nrf2 protein expression induced by OAc-Ph-ADT was significantly inhibited in the presence of LY294002 (Fig. 5G and H). Moreover, the elevated protein expression levels of HO-1, NQO1, and SOD2 induced by OAc-Ph-ADT were also suppressed following the LY294002 treatment (Fig. 5I and J). This suggests that the activation of Nrf2 antioxidant pathway by OAc-Ph-ADT is largely dependent on the regulation of the PI3K/AKT pathway.

3.6. OAc-Ph-ADT upregulates CBS through the Nrf2

CBS is a key enzyme in the transsulfuration pathway, which catalyzes the condensation of homocysteine with serine to produce cystathionine. To validate the role of CBS in endogenous H_2S production, we introduced the commonly used CBS inhibitor AOAA, detected H_2S production using the AzMC probe. As shown in Fig S7, results indicate that endogenous hydrogen sulfide levels in HaCaT cells gradually decreased with increasing AOAA dosage, demonstrating that CBS can regulate endogenous hydrogen sulfide production to a certain extent. Nrf2 is a key transcription factor in the oxidative stress response and regulates CBS expression (Liu et al., 2020). OAc-Ph-ADT increased the expression of CBS in HaCaT cells (Fig. 6A and B). The addition of Brusatol, an inhibitor of Nrf2, decreased both protein and mRNA levels of CBS that were upregulated by OAc-Ph-ADT (Fig. 6C-E). To validate the rergulatory role of Nrf2 on CBS expression, we performed siRNA knockdown of Nrf2. The result revealed that siRNA transfection targeting Nrf2 significantly reduced CBS expression and mRNA levels (Fig. S8). These findings indicate a critical regulatory role of Nrf2 in OAc-Ph-ADT-induced CBS expression.

4. Discussion

Antioxidant stress plays a crucial role in diabetic wound healing. T2DM patients often experience elevated levels of oxidative stress due to a chronic hyperglycemic state, which negatively impacts both the rate and quality of wound healing (Deng et al., 2021; Kido et al., 2017). The persistent hyperglycemic state in diabetic patients triggers oxidative stress, and studies have shown that hyperglycemia-induced ROS accumulation promotes Keap1-dependent ubiquitination degradation of Nrf2 and inhibits its nuclear translocation. Moreover, insulin resistance leads to reduced IRS-1/2 tyrosine phosphorylation, which attenuates PI3K/AKT signaling, and reduced AKT activity dephosphorylates GSK-3β and promotes Nrf2 phosphorylation degradation. Together, these alterations lead to downregulation of the expression of antioxidant enzymes such as HO-1 and NQO1, making cells more vulnerable to oxidative damage (Allen et al., 2005).

Oridonin has a wide range of pharmacological activities and development potential (Li et al., 2021; Zhang et al., 2020), and a series of H_2S-releasing oridonin derivatives were synthesized by structural modification to overcome its low solubility and poor bioavailability (Zhang et al., 2020). In the current study, we established a HaCaT cell model in a high-glucose and high-fat environment, and screened a series of pre-synthesized H_2S-releasing oridonin conjugates by CCK8 assay. OAc-Ph-ADT showed the highest cellular activity and the strongest H_2S-releasing ability, and was chosen for the subsequent study.

The effect of OAc-Ph-ADT on the apoptosis and migration of HaCaT cells were further determined. By inhibiting apoptosis, OAc-Ph-ADT may help retain a greater number of cells involved in the healing process, thus accelerating wound healing. Flow cytometry analysis revealed that apoptosis was elevated in HaCaT cells exposed to high-glucose and high-fat environment, this effect was mitigated by the addition of OAc-Ph-ADT. Furthermore, western blot assay indicated that the expression of apoptosis-related proteins was increased in the high-glucose and high-fat environment. Specifically, OAc-Ph-ADT reduced the levels of cleaved Caspase 3, cleaved-Caspase 9, and the pro-apoptotic protein Bax, thereby suggesting its protective role against apoptosis.

Exposure of keratinocytes to moderate levels of ROS induces Nrf2 expression. However, high levels of ROS overwhelm the antioxidant capacity of the cells, leading to irreversible damage and apoptosis (Heath, Carbone, 2013). Flow cytometry was utilized to demonstrate that OAc-Ph-ADT effectively reduced ROS generation induced by high-glucose and high-fat environment, thereby alleviating oxidative damage in the cells (Liu et al., 2020). Consequently, this led to a reduction in ROS accumulation. Additionally, OAc-Ph-ADT was found to further decrease MDA levels while increasing the content of GSH and SOD in HaCaT cells (Gao et al., 2021). Meanwhile, OAc-Ph-ADT facilitated the nuclear translocation of Nrf2, resulting in increased mRNA levels and protein expression of downstream antioxidant factors, including HO-1, SOD2, and NQO1 (Gao et al., 2021; Loboda et al., 2016).

OAc-Ph-ADT was also found to activate the PI3K/AKT pathway, which in turn increased the expression of downstream migration and proliferation-related proteins, including mTOR and p-GSK3β. Han's study showed that Nrf2 may be a downstream signaling target of PI3K/AKT in MC3T3-E3 cells (Han et al., 2017). To further explore whether OAc-Ph-ADT affects Nrf2 dissociation through the PI3K/AKT pathway, HaCaT cells were treated with the PI3K inhibitor LY294002, and OAc-Ph-ADT-induced Nrf2 protein expression was significantly suppressed, as well as the protein expression levels of HO-1, NQO1, and SOD2, indicating that OAc-Ph-ADT activated the PI3K/AKT/Nrf2 pathway, increased the translocation of Nrf2 to the nucleus, and enhanced the antioxidant effect of downstream HO-1. It was found that Nrf2 was able to bind to the ARE sequence on the CBS gene and enhance CBS expression (Liu et al., 2020). NaHS is a classical exogenous H_2S donor, and exogenous H_2S was able to increase S-sulfation of Keap1, induce dissociation of Nrf2 from Keap1, and enhance Nrf2 nuclear translocation to promote CBS expression (Corsello et al., 2018; Hassan et al., 2012; Hourihan et al., 2013). To investigate the interaction between Nrf2 and CBS in HaCaT cells, the Nrf2 inhibitor Brusatol was used in the study. Experiments revealed that after treating with Brusatol, both the protein and mRNA levels of CBS in cells treated with OAc-Ph-ADT were downregulated, clearly demonstrating the positive regulatory role of Nrf2 on CBS. HaCaT cells are key effector cells in skin barrier function and oxidative stress responses. This study is the first to establish a functional link between Nrf2 and CBS in this model, providing a new perspective for exploring the role of H_2S in skin pathophysiology, such as antioxidant defense, inflammation, or wound healing.

This study employed the HaCaT cell line to investigate the direct damage mechanism of high-glucose and high-fat environments on keratinocytes. This model offers advantages of stability and high reproducibility. However, the model lacks full differentiation capacity, necessitating cautious extrapolation of results to complex physiological environments. The findings of this study primarily focus on the intrinsic responses of keratinocytes themselves, without encompassing their dynamic interactions with fibroblasts, immune cells, and the extracellular matrix during actual wound healing. Future research could further validate and expand the role of these molecular mechanisms in microenvironments closer to *in vivo* conditions through comparisons with primary cells and the establishment of co-culture systems.

In summary, by continuously releasing H_2S, OAc-Ph-ADT promotes HaCaT cells proliferation and migration, and exerts anti-apoptotic and antioxidant effects, making it a candidate for development into wound dressings or gel formulations with high clinical translation potential. Further validation using primary keratinocytes and wound models in diabetic animals would be required to confirm the role and mechanisms of OAc-Ph-ADT in healing process. Ultimately, these efforts aim to develop a clinically effective and user-friendly topical therapeutic agent for diabetes-induced wound healing disorders.

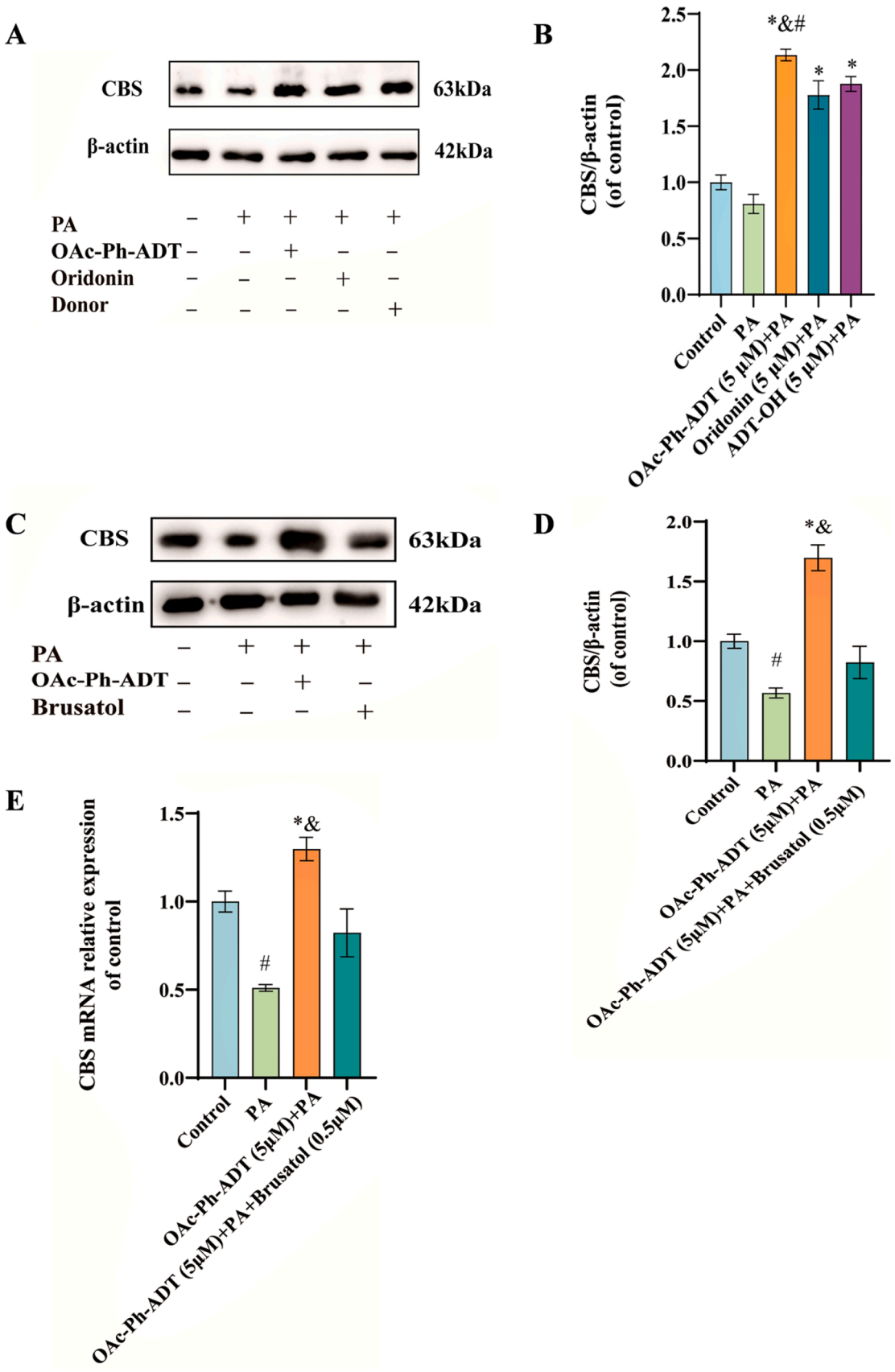

Fig. 6. OAc-Ph-ADT increases CBS expression via regulating Nrf2 in HaCaT cells. (A, B) Western blot analysis of CBS protein levels in different groups. (C-E) The protein expression levels of CBS in each group after the addition of Brusatol were analyzed by western blot, and differences in CBS mRNA content were detected by qPCR. All data were normalized as the optical density ratio between the target protein and β-actin. All results were expressed as the mean ± SD of three independent experiments. $^{\#}P < 0.05$ versus Control; $^{*}P < 0.05$ versus PA group; $^{\&}P < 0.05$ versus Conjugate+ PA+ Brusatol group.

Author statement

The authors declare that they have no known competing financial interests or personal relationships that could have appeared to influence the work reported in this paper. We declare that this' manuscript is original, has not been published before and is not currently being considered for publication elsewhere.

CRediT authorship contribution statement

Yuzhen Jia: Investigation, Formal analysis, Data curation. **Rubing Xue:** Methodology, Investigation, Formal analysis. **Lang Lin:** Writing – original draft, Validation, Resources, Formal analysis, Conceptualization. **Chun Chu:** Writing – review & editing, Visualization, Supervision, Software, Funding acquisition, Data curation. **Fanxing Xu:** Writing – review & editing, Visualization, Validation, Software, Methodology, Funding acquisition, Formal analysis, Conceptualization. **Yutong Shi:** Investigation, Formal analysis, Data curation. **Dahong Li:** Investigation, Data curation.

Declaration of Competing Interest

The authors declare that they have no known competing financial interests or personal relationships that could have appeared to influence the work reported in this paper.

Acknowledgement

This work was funded by the Liaoning Provincial Science and Technology Programme Joint Project (General Program of Natural Science Foundation of Liaoning Province) (Grant Numbers 2024-MSLH-452, 2024-MSLH-425) and the Educational Department of Liaoning Province (LJ212510163005).

Appendix A. Supporting information

Supplementary data associated with this article can be found in the online version at doi:10.1016/j.molimm.2025.12.012.

Data availability

Data will be made available on request.

References

Agostinis, C., Spazzapan, M., Vuerich, R., Balduit, A., Stocco, C., Mangogna, A., Bulla, R., 2021. Differential capability of clinically employed dermal regeneration scaffolds to support vascularization for tissue bioengineering. Biomedicines 9 (10), 1458.

Allen, D.A., Yaqoob, M.M., Harwood, S.M., 2005. Mechanisms of high glucose-induced apoptosis and its relationship to diabetic complications. J. Nutr. Biochem. 16 (12), 705–713.

Cai, F., Xu, H., Cao, N., Zhang, X., Liu, J., Lu, Y., Chen, J., Yang, Y., Cheng, J., Hua, Z.C., Zhuang, H., 2020. ADT-OH, a hydrogen sulfide-releasing donor, induces apoptosis and inhibits the development of melanoma in vivo by upregulating FADD. Cell Death Dis. 11 (1), 33.

Calvert, J.W., Jha, S., Gundewar, S., Elrod, J.W., Ramachandran, A., Pattillo, C.B., Kevil, C.G., Lefer, D.J., 2009. Hydrogen sulfide mediates cardioprotection through Nrf2 signaling. Circ. Res. 105 (4), 365–374.

Chen, J., Mu, Z., Chen, D., Huang, C., Jin, T., Li, L., Cai, X., 2023. H_2S-releasing versatile hydrogel dressing with potent antimicrobial, anti-inflammatory, epithelialization and angiogenic capabilities for diabetic wound healing. Chem. Eng. J. 469, 143985.

Cheng, Z., Garikipati, V.N., Nickoloff, E., Wang, C., Polhemus, D.J., Zhou, J., Benedict, C., Khan, M., Verma, S.K., Rabinowitz, J.E., Lefer, D., Kishore, R., 2016. Restoration of hydrogen sulfide production in diabetic mice improves reparative function of bone marrow cells. Circulation 134 (19), 1467–1483.

Corsello, T., Komaravelli, N., Casola, A., 2018. Role of hydrogen sulfide in Nrf2- and sirtuin-dependent maintenance of cellular redox balance. Antioxidants 7 (10), 129.

Czikora, Á., Erdélyi, K., Ditrói, T., Szántó, N., Jurányi, E.P., Szanyi, S., Tóvári, J., Strausz, T., Nagy, P., 2022. Cystathionine β-synthase overexpression drives metastatic dissemination in pancreatic ductal adenocarcinoma via inducing epithelial-to-mesenchymal transformation of cancer cells. Redox Biol. 57, 102505.

Deng, L., Du, C., Song, P., Chen, T., Rui, S., Armstrong, D.G., Deng, W., 2021. The role of oxidative stress and antioxidants in diabetic wound healing. Oxid. Med. Cell. Longev. 2021, 8852759.

DeNicola, G.M., Karreth, F.A., Humpton, T.J., Gopinathan, A., Wei, C., Frese, K., Mangal, D., Yu, K.H., Yeo, C.J., Calhoun, E.S., Scrimieri, F., Winter, J.M., Hruban, R. H., Iacobuzio-Donahue, C., Kern, S.E., Blair, I.A., Tuveson, D.A., 2011. Oncogene-induced Nrf2 transcription promotes ROS detoxification and tumorigenesis. Nature 475 (7354), 106–109.

Duan, C., Wang, H., Jiao, D., Geng, Y., Wu, Q., Yan, H., Li, C., 2022. Curcumin restrains oxidative stress of after intracerebral hemorrhage in rat by activating the Nrf2/HO-1 pathway. Front. Pharm. 13, 889226.

Gao, X., Xu, D., Zhang, X., Zhao, H., 2021. Protective effect of lemon peel polyphenols on oxidative stress-induced damage to human keratinocyte HaCaT cells through activation of the Nrf2/HO-1 signaling pathway. Front. Nutr. 7, 606776.

Han, D., Chen, W., Gu, X., Shan, R., Zou, J., Liu, G., Shahid, M., Gao, J., Han, B., 2017. Cytoprotective effect of chlorogenic acid against hydrogen peroxide-induced oxidative stress in MC3T3-E1 cells through PI3K/Akt-mediated Nrf2/HO-1 signaling pathway. Oncotarget 8 (9), 14680–14692.

Hassan, M.I., Boosen, M., Schaefer, L., Kozlowska, J., Eisel, F., von Knethen, A., Beck, M., Hemeida, R.A., El-Moselhy, M.A., Hamada, F.M., Beck, K.F., Pfeilschifter, J., 2012. Platelet-derived growth factor-BB induces cystathionine γ-lyase expression in rat mesangial cells via a redox-dependent mechanism. Br. J. Pharmacol. 166 (8), 2231–2242.

He, Y., Sun, M.M., Zhang, G.G., Yang, J., Chen, K.S., Xu, W.W., Li, B., 2021. Targeting PI3K/Akt signal transduction for cancer therapy. Signal Transduct. Target Ther. 6 (1), 425.

Heath, W.R., Carbone, F.R., 2013. The skin-resident and migratory immune system in steady state and memory: innate lymphocytes, dendritic cells and T cells. Nat. Immunol. 14 (10), 978–985.

Hourihan, J.M., Kenna, J.G., Hayes, J.D., 2013. The gasotransmitter hydrogen sulfide induces nrf2-target genes by inactivating the keap1 ubiquitin ligase substrate adaptor through formation of a disulfide bond between cys-226 and cys-613. Antioxid. Redox. Signal. 19 (5), 465–481.

Huerta de la Cruz, S., Rodríguez-Palma, E.J., Santiago-Castañeda, C.L., Beltrán-Ornelas, J.H., Sánchez-López, A., Rocha, L., Centurión, D., 2022. Exogenous hydrogen sulfide restores CSE and CBS but no 3-MST protein expression in the hypothalamus and brainstem after severe traumatic brain injury. Metab. Brain Dis. 37 (6), 1863–1874.

Jin, H., Zhang, Z., Wang, C., Tang, Q., Wang, J., Bai, X., Wang, Q., Nisar, M., Tian, N., Wang, Q., Mao, C., Zhang, X., Wang, X., 2018. Melatonin protects endothelial progenitor cells against AGE-induced apoptosis via autophagy flux stimulation and promotes wound healing in diabetic mice. Exp. Mol. Med. 50 (11), 1–15.

Kabil, O., Motl, N., Banerjee, R., 2014. H_2S and its role in redox signaling. Biochim. Biophys. Acta. 1844 (8), 1355–1366.

Khodr, B., Khalil, Z., 2001. Modulation of inflammation by reactive oxygen species: implications for aging and tissue repair. Free Radic. Biol. Med. 30 (1), 1–8.

Kido, D., Mizutani, K., Takeda, K., Mikami, R., Matsuura, T., Iwasaki, K., Izumi, Y., 2017. Impact of diabetes on gingival wound healing via oxidative stress. PloS One 12 (12), e0189601.

Lan, C.C., Liu, I.H., Fang, A.H., Wen, C.H., Wu, C.S., 2008. Hyperglycaemic conditions decrease cultured keratinocyte mobility: implications for impaired wound healing in patients with diabetes. Br. J. Dermatol. 159 (5), 1103–1115.

Li, Z.G., 2015. Quantification of hydrogen sulfide concentration using methylene blue and 5,5′-dithiobis(2-nitrobenzoic acid) methods in plants. Methods Enzym. 554, 101–110.

Li, L., Cheng, S.Q., Guo, W., Cai, Z.Y., Sun, Y.Q., Huang, X.X., Yang, J., Ji, J., Chen, Y.Y., Dong, Y.F., Cheng, H., Sun, X.L., 2021. Oridonin prevents oxidative stress-induced endothelial injury via promoting Nrf-2 pathway in ischaemic stroke. J. Cell. Mol. Med. 25 (20), 9753–9766.

Li, H., Gao, X., Huang, X., Wang, X., Xu, S., Uchita, T., Gao, M., Xu, J., Hua, H., Li, D., 2019. Hydrogen sulfide donating ent-kaurane and spirolactone-type 6,7-seco-ent-kaurane derivatives: design, synthesis and antiproliferative properties. Eur. J. Med. Chem. 178, 446–457.

Li, H., Ma, Q., Jia, Y., Wang, C., Wu, J., Wang, S., Hua, H., Lu, J., Li, D., 2024. H_2S-releasing oridonin derivatives with improved antitumor activity by inhibiting the PI3K/AKT pathway. Bioorg. Med. Chem. 115, 117968.

Li, H., Mu, J., Sun, J., Xu, S., Liu, W., Xu, F., Li, D., 2020. Hydrogen sulfide releasing oridonin derivatives induce apoptosis through extrinsic and intrinsic pathways. Eur. J. Med. Chem. 187, 111978.

Li, X., Zhang, C.T., Ma, W., Xie, X., Huang, Q., 2021. Oridonin: a review of its pharmacology, pharmacokinetics and toxicity. Front. Pharmacol. 12, 645824.

Liang, Y., Yang, C., Lin, Y., Parviz, Y., Sun, K., Wang, W., Ren, M., Yan, L., 2019. Matrix metalloproteinase 9 induces keratinocyte apoptosis through FasL/Fas pathway in diabetic wound. Apoptosis 24 (7-8), 542–551.

Liu, N., Lin, X., Huang, C., 2020. Activation of the reverse transsulfuration pathway through NRF2/CBS confers erastin-induced ferroptosis resistance. Br. J. Cancer 122 (2), 279–292.

Liu, H., Zhang, Z., Zhang, L., Yao, X., Zhong, X., Cheng, G., Wang, L., Wan, Q., 2020. Spiraeoside protects human cardiomyocytes against high glucose-induced injury, oxidative stress, and apoptosis by activation of PI3K/Akt/Nrf2 pathway. J. Biochem. Mol. Toxicol. 34 (10), e22548.

Loboda, A., Damulewicz, M., Pyza, E., Jozkowicz, A., Dulak, J., 2016. Role of Nrf2/HO-1 system in development, oxidative stress response and diseases: an evolutionarily conserved mechanism. Cellular and molecular life sciences. Cell. Mol. Life Sci. 73 (17), 3221–3247.

Mironov, A., Seregina, T., Nagornykh, M., Luhachack, L.G., Korolkova, N., Lopes, L.E., Kotova, V., Zavilgelsky, G., Shakulov, R., Shatalin, K., Nudler, E., 2017. Mechanism of H_2S-mediated protection against oxidative stress in *Escherichia coli*. Proc. Natl. Acad. Sci. 114 (23), 6022–6027.

Mohan, M., Al-Talabany, S., McKinnie, A., Mordi, I.R., Singh, J.S.S., Gandy, S.J., Baig, F., Hussain, M.S., Bhalraam, U., Khan, F., Choy, A.M., Matthew, S., Houston, J.G., Struthers, A.D., George, J., Lang, C.C., 2019. A randomized controlled trial of metformin on left ventricular hypertrophy in patients with coronary artery disease without diabetes: the MET-REMODEL trial. Eur. Heart J. 40 (41), 3409–3417.

O'Rourke, S.A., Shanley, L.C., 2024. The Nrf2-HO-1 system and inflammaging. Front. Immunol. 15, 1457010.

Peake, B.F., Nicholson, C.K., Lambert, J.P., Hood, R.L., Amin, H., Amin, S., Calvert, J.W., 2013. Hydrogen sulfide preconditions the db/db diabetic mouse heart against ischemia-reperfusion injury by activating Nrf2 signaling in an Erk-dependent manner. Am. J. Physiol. Heart Circ. Physiol. 304 (9), H1215–H1224.

Powell, C.R., Dillon, K.M., Matson, J.B., 2018. A review of hydrogen sulfide (H_2S) donors: Chemistry and potential therapeutic applications. Biochem. Pharmacol. 149, 110–123.

Qian, Y., Altamimi, A., Yates, S.A., Sarkar, S., Cochran, M., Zhou, M., Levi-Polyachenko, N., Matson, J.B., 2020. H_2S-releasing amphiphilic dipeptide hydrogels are potent S. aureus biofilm disruptors. Biomater. Sci. 8 (9), 2564–2576.

Scheid, S., Goeller, M., Baar, W., Wollborn, J., Buerkle, H., Schlunck, G., Lagrèze, W., Goebel, U., Ulbrich, F., 2021. Hydrogen sulfide reduces ischemia and reperfusion injury in neuronal cells in a dose- and time-dependent manner. Int J. Mol. Sci. 22 (18), 10099.

Schlienger, J.L., 2013. Complications du diabète de type 2 [Type 2 diabetes complications]. La Presse Médicale 42 (5), 839–848 (Paris. France : 1983).

Sies, H., Berndt, C., Jones, D.P., 2017. Oxidative Stress. Annu. Rev. Biochem. 86, 715–748.

Song, M., Liu, X., Liu, K., Zhao, R., Huang, H., Shi, Y., Zhang, M., Zhou, S., Xie, H., Chen, H., Li, Y., Zheng, Y., Wu, Q., Liu, F., Li, E., Bode, A.M., Dong, Z., Lee, M.H., 2018. Targeting AKT with oridonin inhibits growth of esophageal squamous cell carcinoma i*n vitro* and patient-derived xenografts i*n vivo*. Mol. Cancer. Ther. 17 (7), 1540–1553.

Szabo, C., 2016. Gasotransmitters in cancer: from pathophysiology to experimental therapy. Nat. Rev. Drug Discov. 15 (3), 185–203.

Wang, M., Chen, X., Qu, Y., Ma, Q., Pan, H., Li, H., Hua, H., Li, D., 2023. Design and synthesis of brefeldin A-Isothiocyanate derivatives with selectivity and their potential for cervical cancer therapy. Molecules. 28 (11), 4284.

Werge, M.P., McCann, A., Galsgaard, E.D., Holst, D., Bugge, A., Albrechtsen, N.J.W., Gluud, L.L., 2021. The role of the transsulfuration pathway in non-alcoholic fatty liver disease. J. Clin. Med. 10 (5), 1081.

Xie, L., Gu, Y., Wen, M., Zhao, S., Wang, W., Ma, Y., Meng, G., Han, Y., Wang, Y., Liu, G., Moore, P.K., Wang, X., Wang, H., Zhang, Z., Yu, Y., Ferro, A., Huang, Z., Ji, Y., 2016. Hydrogen sulfide induces Keap1 S-sulfhydration and suppresses diabetes-accelerated atherosclerosis via Nrf2 activation. Diabetes. 65 (10), 3171–3184.

Xu, F., Gao, X., Li, H., Xu, S., Li, X., Hu, X., Li, Z., Xu, J., Hua, H., Li, D., 2019. Hydrogen sulfide releasing enmein-type diterpenoid derivatives as apoptosis inducers through mitochondria-related pathways. Bioorg. Chem. 82, 192–203.

Zhang, H., Chen, N., 2022. Adropin as an indicator of T2DM and its complications. Food Sci. Hum. Wellness 11 (6), 1455–1463.

Zhang, Y., Wang, S., Dai, M., Nai, J., Zhu, L., Sheng, H., 2020. Solubility and bioavailability enhancement of oridonin: a review. Molecules. 25 (2), 332.

Zhang, Z., Wu, X., Kong, Y., Zou, P., Wang, Y., Zhang, H., Cui, G., Zhu, W., Chen, H., 2024. Dynamic changes and effects of H_2S, IGF-1, and GH in the traumatic brain injury. Biochem. Genet. 62 (5), 3821–3840.

Zhang, Y.P., Zhang, Q., Deng, F., Chen, B., Zhang, J.H., Hu, J., 2022. Effect of P62 on the migration and motility of human epidermal cell line HaCaT in high glucose microenvironment and its mechanism. Chin. J. Burns Wounds 38 (11), 1014–1022.

Zhou, X., An, G., Chen, J., 2014. Inhibitory effects of hydrogen sulphide on pulmonary fibrosis in smoking rats via attenuation of oxidative stress and inflammation. J. Cell Mol. Med. 18 (6), 1098–1103.

Zhu, H., Blake, S., Chan, K.T., Pearson, R.B., Kang, J., 2018. Cystathionine β-synthase in physiology and cancer. Biomed. Res. Int., 3205125